REPORT DOCUMENTATION PAGE

AFRL-SR-AR-TR-05-

0373

1. AGENCY USE ONLY (Leave blank)	2. REPORT DATE	3. REPORT TYPE AND DATES COVERED
	July 20, 2005	Final Report 01/01/2003 to 03/31/2005

4. TITLE AND SUBTITLE
"Algorithm Development for the Two-Fluid Plasma Model"

5. FUNDING NUMBERS
F49620-02-1-0129

6. AUTHOR(S)
Dr Uri Shumlak

7. PERFORMING ORGANIZATION NAME(S) AND ADDRESS(ES)

University of Washington
Office of Sponsored Programs
Box 354945
Seattle, WA 98195-4945

8. PERFORMING ORGANIZATION REPORT NUMBER
Final 62-6759

9. SPONSORING / MONITORING AGENCY NAME(S) AND ADDRESS(ES)

USAF, AFRL
AF Office of Scientific Research
4015 Wilson Blvd, Room 713
Arlington, VA 22203-1954
Beverly Sivels, (703) 696-9732

NM

10. SPONSORING / MONITORING AGENCY REPORT NUMBER

11. SUPPLEMENTARY NOTES

12a. DISTRIBUTION / AVAILABILITY STATEMENT
No distribution/avaiability restrictions noted at this time.

Approved for public release;
distribution unlimited

12b. DISTRIBUTION CODE

13. ABSTRACT *(Maximum 200 Words)*

A new algorithm is developed based on the complete two-fluid plasma model. The model captures physics that is not contained in the more commom magnetohydrodynamic model. Recent progress on the algorithm development for the two-fluid plasama model includes analysis of the simulation results, extension to two two dimensions, and preliminary investigation of a higher order method. The algorithm is first developed in one dimension and applied to the electromagnetic plasma shock. Results are analyzed to provide physical support for the numerically observed fast waves. The two-fluid plasma algorithm is extended to multidimensions including a complete electromagnetic field description. The divergence constraints on the fields are satisfied by transforming the constraints into hyperbolic equations. A preliminary higher-order discontinuous Galerkin, Runge-Kutta method is investigated to more accurately balance equilibrium sources.

14. SUBJECT TERMS
Algorithms, Two Fluid Plasma

15. NUMBER OF PAGES
21

16. PRICE CODE

17. SECURITY CLASSIFICATION OF REPORT	18. SECURITY CLASSIFICATION OF THIS PAGE	19. SECURITY CLASSIFICATION OF ABSTRACT	20. LIMITATION OF ABSTRACT
U	U	U	UU

Final Performance Report (1/1/03 – 3/31/05)

AFOSR Grant No. F49620-02-1-0129

"ALGORITHM DEVELOPMENT FOR THE TWO-FLUID PLASMA MODEL"

Submitted to

Air Force Office of Scientific Research / NM
4015 Wilson Boulevard, Room 713
Arlington, VA 22203-1954

University of Washington
Department of Aeronautics and Astronautics
Aerospace & Energetics Research Program
Box 352250
Seattle, WA 98195-2250

Dr. Uri Shumlak
Principal Investigator

7/20/05

ALGORITHM DEVELOPMENT FOR THE TWO-FLUID PLASMA MODEL

AFOSR Grant No. F49620-02-1-0129

U. Shumlak

Department of Aeronautics and Astronautics
Aerospace & Energetics Research Program
University of Washington

Abstract

A new algorithm is developed based on the complete two-fluid plasma model. The model captures physics that is not contained in the more common magnetohydrodynamic model. Recent progress on the algorithm development for the two-fluid plasma model includes analysis of the simulation results, extension to two dimensions, and preliminary investigation of a higher order method. The algorithm is first developed in one dimension and applied to the electromagnetic plasma shock. Results are analyzed to provide physical support for the numerically observed fast waves. The two-fluid plasma algorithm is extended to multidimensions including a complete electromagnetic field description. The divergence constraints on the fields are satisfied by transforming the constraints into hyperbolic equations. A preliminary higher-order discontinuous Galerkin, Runge-Kutta method is investigated to more accurately balance equilibrium sources.

1 Executive Summary

This project represents a three year effort to develop a new algorithm for plasma simulations based on the two-fluid plasma model. Current plasma simulation algorithms capable of complex geometries are based on the MHD (magnetohydrodynamic) model. The derivation of the MHD model involves several assumptions that severely limit its applicability. The two-fluid model only assumes local thermodynamic equilibrium and is, therefore, more physically accurate and capable than MHD models. The two-fluid model is formulated in conservation form. An approximate Riemann solver is developed for the two-fluid plasma model to compute the fluxes in a stable and accurate manner. Several methods are investigated to solve the electromagnetic field model, which includes the source terms and divergence constraints. These methods include a characteristic-based algorithm, a perfectly hyperbolic modification, and a mixed potential formulation. The two plasma fluids and the electromagnetic fields communicate through the source terms. The fluid momentum and

energy equations have source terms that depend on $\mathbf{E}$ and $\mathbf{B}$. The electromagnetic equations have source terms that depend on $\mathbf{v}_i$ and $\mathbf{v}_e$ (Ampere's law) and n_i and n_e (Poisson's equation). Accurately coupling the source terms is important both for numerical stability and for modeling plasmas where large equilibrium forces exist.

An algorithm is developed for the complete two-fluid plasma model initially in one dimension. The algorithm uses a Roe-type approximate Riemann solver [1] to discretize the hyperbolic fluxes of the fluid model and an upwind characteristic-based solver for the electromagnetic fields. Simulations from the resulting finite volume algorithm are benchmarked against known analytical results. Furthermore, the algorithm is applied to the electromagnetic plasma shock problem to reveal the transition from gas dynamic shock to MHD shock. The results are analyzed to reveal the fast plasma waves that are captured in the two-fluid plasma model. [2]

The algorithm is extended to multiple dimensions. The divergence constraints can be difficult to satisfy with the presence of current and charge sources on an arbitrary computational grid. The divergence constraints are satisfied by reformulating Maxwell's equations to include correction potentials. The approach involves coupling the divergence constraint equations with the time-dependent field equations to form a perfectly hyperbolic equation set. [3] The finite volume algorithm is applied to a two-dimensional plasma shock problem which is similar to a field reversed configuration (FRC) being investigated at the Air Force Research Laboratories (FRC magnetic implosions). The simulations demonstrate the importance of accurately modeling the source terms. The FRC simulation must balance large magnetic field forces with large plasma pressure forces. A preliminary algorithm is developed using a discontinuous Galerkin method. [4].

This project resulted in the Master of Science theses for Chris Aberle and John Loverich titled "Algorithm for Solving Colocated Electromagnetic Fields with Sources" and "A Finite Volume Algorithm for the Two-fluid Plasma System in One Dimension", respectively. Archival journal and conference papers were published reporting on the work from this project. Archival journal papers are U. Shumlak, J. Loverich, "Approximate Riemann solver for the two-fluid plasma model", Journal of Computational Physics **187**, 620-638 (2003) and "A discontinuous Galerkin method for the full two-fluid plasma model", Computer Physics Communications **169** 251-255 (2005). This project was performed by Prof. Uri Shumlak and graduate students Chris Aberle, Ammar Hakim, and John Loverich.

2 Project Description

Plasmas are essential to many technologies that are important to the Air Force, some of which have dual-use potential. These applications include portable pulsed power systems, high power microwave devices, drag reduction for hyper-

sonic vehicles, advanced plasma thrusters for space propulsion, nuclear weapons effects simulations, radiation production for counter proliferation, and fusion for power generation. Several of these applications are specifically mentioned in the *New World Vistas* Report from the USAF Scientific Advisory Board. [5] In general, plasmas fall into a density regime where they exhibit both collective (fluid) behavior and individual (particle) behavior. The intermediate regime complicates the computational modeling of plasmas.

2.1 Kinetic, PIC, and MHD Models

Plasmas may be most accurately modeled using kinetic theory. The plasma is described by distribution functions in physical space, velocity space, and time, $f(\mathbf{x}, \mathbf{v}, t)$. The evolution of the plasma is then modeled by the Boltzmann equation.

$$\frac{\partial f_\alpha}{\partial t} + \mathbf{v}_\alpha \cdot \frac{\partial f_\alpha}{\partial \mathbf{x}} + \frac{q_\alpha}{m_\alpha} (\mathbf{E} + \mathbf{v}_\alpha \times \mathbf{B}) \cdot \frac{\partial f_\alpha}{\partial \mathbf{v}} = \left.\frac{\partial f_\alpha}{\partial t}\right|_{collisions} \tag{1}$$

for each plasma species α = ions, electrons. The Boltzmann equation coupled with Maxwell's equations for electromagnetic fields completely describe the plasma dynamics. [6–8] However, the Boltzmann equation is seven dimensional. As a consequence of the large dimensionality plasma simulations using the Boltzmann equation are only used in very limited applications with narrow distributions, small spatial extent, and short time durations. [9, 10] The seven dimensional space is further exacerbated by the high velocity space that is unused except for tail of the distribution or energetic beams. Boundary conditions are difficult to implement in kinetic simulations.

Particle in cell (PIC) plasma model apply the Boltzmann equation to representative superparticles which are far fewer (10^7) than the number of particles in the actual plasma (10^{20}). [11] PIC simulations have similar limitations as simulations using kinetic theory due to statistical errors caused by the fewer superparticles. Boundary conditions are also difficult to implement in PIC simulations.

The other end of the spectrum in plasma model involves taking moments of the Boltzmann equation and averaging over velocity space for each species which implicitly assumes local thermodynamic equilibrium. The resulting equations comprise the two-fluid plasma model. The two-fluid equations are then combined to form the MHD model. [12] However, in the process several approximations are made which limit the applicability of the MHD model to low frequency and ignores the electron mass and finite Larmor radius effects.

The MHD model treats the plasma like a conducting fluid and assigning macroscopic parameters to describe its particle-like interactions. Plasma simulation algorithms based on the MHD model have been very successful in modeling plasma dynamics and other phenomena. Codes such as MACH2 are based on arbitrary Lagrangian/Eulerian formulations. [13] ALE codes are well suited for simulating plasma phenomena involving moving interfaces. [14] However,

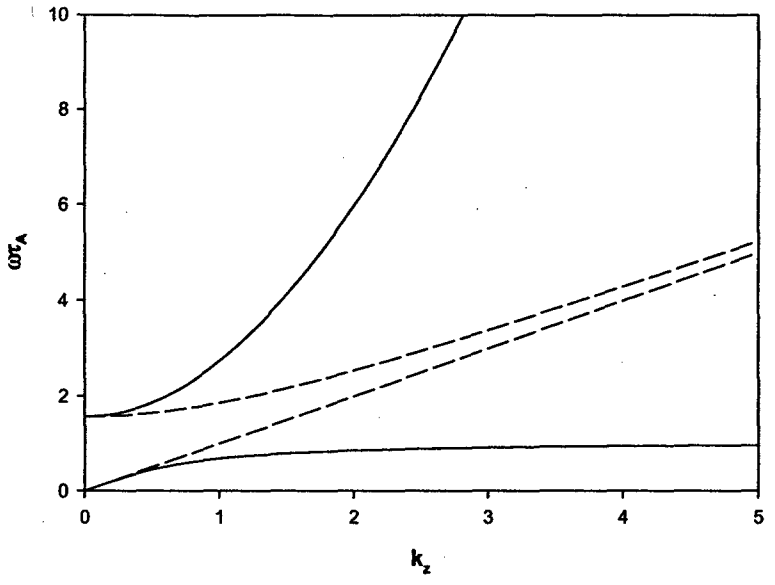

Figure 1: Dispersion relation for the fast and slow modes with $\omega_c\tau = 1.0$. The dashed lines represent the ideal MHD modes.

ALE codes cannot be formulated as conservation laws and lack many of the inherent conservative properties. The MHD model has been successfully implemented in conservative form to simulate realistic three-dimensional geometries. [15, 16]

A severe limitation of the MHD model is the treatment the Hall effect and diamagnetic terms. These terms represent the separate motions of the ions and electrons. The Hall effect and diamagnetic terms also account for ion current and the finite ion Larmor radius. These effects are important in many applications such as electric space propulsion thrusters: Hall thrusters, magnetoplasmadynamic (MPD) thrusters, Lorentz force thrusters. The Hall term is also believed to be important to electrode effects such as anode and cathode fall which greatly affect many directly coupled plasma applications. Furthermore, the Hall and diamagnetic effects may be important for hypersonic flow applications. [17]

The Hall terms can be difficult to stabilize because they lead to the whistler wave branch of the dispersion relation. The phase and group velocities of the whistler wave increase with frequency. The velocities become large even for modest values of the Hall parameter. See Fig. 1 for the dispersion diagram for a modest value of the Hall parameter ($\omega_c\tau = 1$).

A semi-implicit technique has been applied to treat the Hall term. [18, 19] After the hyperbolic terms of the MHD equations are advanced, the Hall terms are treated independently. The conserved variables are then corrected. The procedure can be computationally intensive. The operator stencil uses 5 points in the sweep direction and 3 points in each orthogonal direction. The complete

operator stencil is 45 points. The semi-implicit method works adequately for small Hall parameters, but becomes unstable or slow to converge for the large Hall parameters often seen in applications.

2.2 Project Results

The next step is to extend the realistic geometry capabilities of the MHD model to the more physically accurate two-fluid model. The complexity of the two-fluid model is greater the MHD model but significantly less than the kinetic model.

In this project a new algorithm is developed that solves the two-fluid plasma model using an approximate Riemann solver. [2] The method tracks the wave propagation across the domain based on conservation laws.

The two-fluid plasma model captures the separate motion of the electrons and ions without the added complexity of the kinetic model. The two-fluid model is derived by taking moments of the Boltzmann equation for each species. The process of taking moments eliminates the velocity space and yields representative fluid variables (density, momentum, energy) for each species. The only approximation made is local thermodynamic equilibrium within each fluid and is, therefore, a generalization of the MHD model. The fundamental variables are generated by taking moments of the distribution function.

The evolution of the particle density of the ions and electrons is expressed by continuity equations. The equations are the zeroth moment of the Boltzmann equation.

$$\frac{\partial n_i}{\partial t} + \nabla \cdot \left(\frac{\mathbf{j}_i}{q} \right) = 0 \tag{2}$$

$$\frac{\partial n_e}{\partial t} - \nabla \cdot \left(\frac{\mathbf{j}_e}{e} \right) = 0 \tag{3}$$

where n_i, n_e are the ion and electron number densities and the particle fluxes are defined by the partial current densities $\mathbf{j}_i = q n_i \mathbf{v}_i$ and $\mathbf{j}_e = -e n_e \mathbf{v}_e$ in terms of the charges q, e and fluid velocities $\mathbf{v}_i$, $\mathbf{v}_e$ for the ion and electron fluids.

The first moment of the Boltzmann equation yields momentum equations for each species. The momentum equations are written in divergence form.

$$\frac{\partial \mathbf{j}_i}{\partial t} + \nabla \cdot \left(\frac{\mathbf{j}_i \mathbf{j}_i}{q n_i} + \frac{q}{m_i} p_i \mathbf{I} \right) = \frac{q^2 n_i}{m_i} \mathbf{E} + \frac{q}{m_i} \mathbf{j}_i \times \mathbf{B} + \frac{q}{m_i} \mathbf{R}_{ei} \tag{4}$$

$$\frac{\partial \mathbf{j}_e}{\partial t} - \nabla \cdot \left(\frac{\mathbf{j}_e \mathbf{j}_e}{e n_e} + \frac{e}{m_e} p_e \mathbf{I} \right) = \frac{e^2 n_e}{m_e} \mathbf{E} - \frac{e}{m_e} \mathbf{j}_e \times \mathbf{B} + \frac{e}{m_e} \mathbf{R}_{ei} \tag{5}$$

where $\mathbf{E}$ and $\mathbf{B}$ are the electric and magnetic fields, p_i and p_e are the ion and electron partial pressures, and $\mathbf{R}_{ei}$ is the electron to ion momentum transfer vector.

The second moment of the Boltzmann equation yields energy equations for each species which are expressed in divergence form for the total energy.

$$\frac{\partial \varepsilon_i}{\partial t} + \nabla \cdot \left[(\varepsilon_i + p_i) \frac{\mathbf{j}_i}{e n_i} \right] = \mathbf{j}_i \cdot \left(\mathbf{E} + \frac{\mathbf{R}_{ei}}{e n_i} \right) \tag{6}$$

$$\frac{\partial \varepsilon_e}{\partial t} - \nabla \cdot \left[(\varepsilon_e + p_e) \frac{\mathbf{j}_e}{e n_e} \right] = \mathbf{j}_e \cdot \left(\mathbf{E} + \frac{\mathbf{R}_{ei}}{e n_e} \right) \tag{7}$$

where the total energy is defined by

$$\varepsilon_i \equiv \frac{1}{\gamma - 1} p_i + \frac{1}{2} n_i m_i v_i^2 \tag{8}$$

and

$$\varepsilon_e \equiv \frac{1}{\gamma - 1} p_e + \frac{1}{2} n_e m_e v_e^2. \tag{9}$$

where γ is the ratio of specific heats and T_i, T_e are the ion and electron temperatures. An adiabatic equation of state is assumed. The temperatures are related to the partial pressures by $p_\alpha = n_\alpha T_\alpha$ for $\alpha = \{i, e\}$.

The equations that govern the ion and electron fluids are rewritten in compact, conservative form.

$$\frac{\partial Q}{\partial t} + \nabla \cdot \mathbf{F} = S \tag{10}$$

where Q is the vector of conserved fluid variables, $\mathbf{F}$ is the tensor of hyperbolic fluxes $(F\hat{x} + G\hat{y} + H\hat{z})$, and S is the vector containing the source terms. The vector of conserved variables is

$$Q = \left[n_i, n_e, j_{i_x}, j_{i_y}, j_{i_z}, j_{e_x}, j_{e_y}, j_{e_z}, \varepsilon_i, \varepsilon_e \right]^T. \tag{11}$$

for the number densities, electrical current densities, and energy densities. The flux Jacobian $\partial F / \partial Q$ for the two fluid equations is constructed in the usual way. The characteristic velocities are calculated to construct the approximate Riemann fluxes.

The eigenvalues of the flux Jacobian give the characteristic velocities.

$$\lambda = \left\{ \frac{j_{i_x}}{e n_i}, \frac{j_{i_x}}{e n_i} \pm \sqrt{\frac{5}{3} \frac{T_i}{m_i}}, -\frac{j_{e_x}}{e n_e}, -\frac{j_{e_x}}{e n_e} \pm \sqrt{\frac{5}{3} \frac{T_e}{m_e}} \right\} \tag{12}$$

The eigenvalues for the two fluid plasma model represent the combination of the drift speeds and thermal speeds for the electrons and ions.

The electromagnetic fields influence the motion of the plasma fluid through the Lorentz force which is contained in eqns(4) and (5). The motion of the plasma influences the evolution of the electromagnetic fields through the redistribution of charge density and current density. Maxwell's equation govern the evolution of the electromagnetic fields. The charge density $qn_i - en_e$ and

current density ($\mathbf{j} = \mathbf{j}_i + \mathbf{j}_e$) are calculated directly from the two-fluid equations which couple the electromagnetic fields.

$$\frac{\partial \mathbf{B}}{\partial t} = -\nabla \times \mathbf{E} \tag{13}$$

$$\epsilon_0 \frac{\partial \mathbf{E}}{\partial t} = \nabla \times \mathbf{B}/\mu_0 - \mathbf{j} \tag{14}$$

$$\epsilon_0 \nabla \cdot \mathbf{E} = q n_i - e n_e \tag{15}$$

$$\nabla \cdot \mathbf{B} = 0 \tag{16}$$

The two-fluid plasma model (including the electromagnetic equations) can also be expressed in divergence form.

$$\frac{\partial Q}{\partial t} + \nabla \cdot \mathbf{F} = S \tag{17}$$

where Q is the vector of conserved fluid variables, $\mathbf{F}$ is the tensor of hyperbolic fluxes ($F\hat{x} + G\hat{y} + H\hat{z}$), and S is the vector containing the source terms.

The hyperbolic fluxes are discretized using a Roe-type approximate Riemann solver. [1] In this method the overall solution is built upon the solutions to the Riemann problem defined by the discontinuous jump in the solution at each cell interface. The numerical flux for a first-order accurate (in space) Roe-type solver is written in symmetric form as

$$F_{i+1/2} = \frac{1}{2}\left(F_{i+1} + F_i\right) - \frac{1}{2}\sum_k l_k \left(Q_{i+1} - Q_i\right) |\lambda_k| \, r_k \tag{18}$$

where r_k is the k^{th} right eigenvector, λ_k is the k^{th} eigenvalue, and l_k is the k^{th} left eigenvector, evaluated at the cell interface $(i + 1/2)$. The values at the cell interface are obtained by a Roe average of the neighboring cells. Higher order accuracy is obtained by using a minmod flux limiter in the numerical flux calculation. The algorithm is second-order accurate in regions where the solution is smooth and first-order accurate in the vicinity of large gradients in the solution. The flux calculated as above is normal to the cell interface which is the desired orientation for applying the divergence theorem in a finite volume method.

The source terms of eqn(17) are large, in general, since they contain the electromagnetic forces that act upon the fluids. The homogeneous fluxes are calculated for the electron and ion fluids with the approximate Riemann solver described previously. An approximate Riemann solver is also used to calculate the homogeneous fluxes for Maxwell's equations. The large source terms make the equation stiff. The source terms for all of the equations are then solved self-consistently with an implicit treatment to alleviate the stiffness of the problem.

$$\left.\frac{\partial Q}{\partial t}\right|_{sources}^{n+1} = S^{n+1} \tag{19}$$

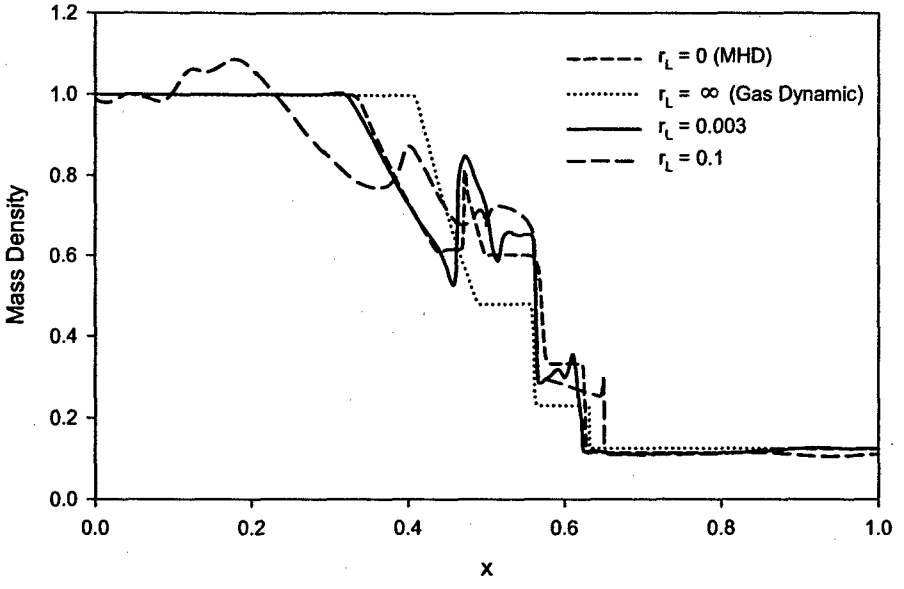

Figure 2: Two-fluid solution of the electromagnetic plasma shock problem for four values of the Larmor radius r_L. The transition from gas dynamic shock to MHD shock is evident. Fast moving waves are present for intermediate values of r_L.

where S^{n+1} is the source term evaluated at the $n+1$ time step. Previously, the source term is expanded in a Taylor series to first order and a Newton iteration is required to solve the equation. This step has been eliminated by using an implicit time approach to rewrite the equation as

$$\left.\frac{\partial Q}{\partial t}\right|_{sources}^{n+1} = S^{n+1} = S^n + \frac{\partial S}{\partial Q}\frac{\partial Q}{\partial t}\Delta t = \left(1 + \frac{\partial S}{\partial Q}\Delta t\right)^{-1} S^n. \qquad (20)$$

This formulation does not require a Newton iteration.

2.2.1 One-Dimensional Algorithm

The described algorithm is used to simulate the coplanar Riemann problem to test for proper wave capturing behavior, Langmuir oscillations to test the electric field component in the Lorentz force, and the electromagnetic plasma shock.

The two-fluid algorithm is benchmarked to the electromagnetic plasma shock problem often used for MHD algorithms as in Ref. [20]. The MHD shock problem is a good test of the two-fluid algorithm's ability to model MHD like problems. MHD problems are characterized by strong coupling of the two-fluid source terms which makes for a stiff system of equations. In this benchmark case, it is shown that the algorithm can be used to model MHD like problems.

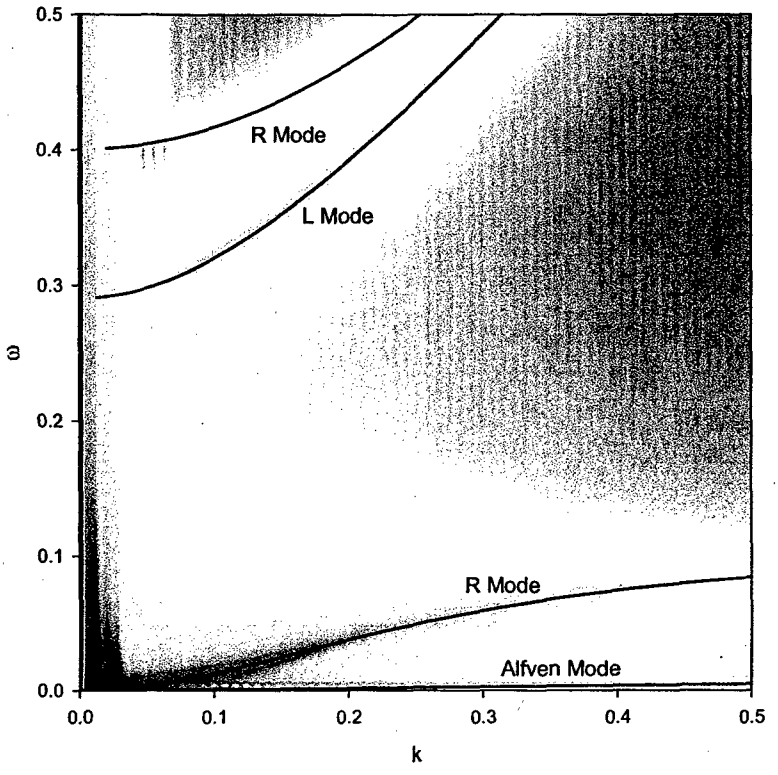

Figure 3: Fourier analysis of the numerical results for a small amplitude electromagnetic plasma shock compared to the analytical dispersion relations for plasma waves for $r_L = 0.1$. Analytical dispersion relations for the L mode, R mode, and Alfvén mode waves are plotted for comparison. The low frequency portion of the lower branch of the R mode is the whistler wave. The agreement of the numerical and analytical results supports the physical basis for the fast waves in the two-fluid solutions.

The comparison is made between the ideal MHD solution and a two-fluid solution with equivalent initial conditions. The two-fluid model allows the flexibility to choose the desired Larmor radius r_L (zero in MHD), the ionic charge state (unity in MHD), and the electron to ion mass ratio (zero in MHD). For the simulations presented here, the ionic charge state is set to one, and the electron to ion mass ratio is set to 5.45×10^{-3} (hydrogen plasma). The Larmor radius is varied while holding the Alfvén and sound speeds constants.

Simulation results are presented in Fig. 2 comparing the results for four values of the Larmor radius. As the Larmor radius decreases, the two-fluid solution approaches the MHD solution. The algorithm is able to capture the MHD shock in the limit of $r_L \to 0$, the gas dynamic shock in the limit of $r_L \to \infty$, and two-fluid (Hall effect) physics for intermediate values. The MHD model assumes $r_L = 0$ where the electron and ion fluids are tightly coupled to

the magnetic field. The plasma completely decouples from the magnetic field when $r_L = \infty$. The transition from gas dynamic shock to MHD shock is a smooth transition that shows faster moving waves for intermediate values of the Larmor radius and has not been previously studied.

Simulation results reveal the transition from gas dynamic shock to MHD shock is a smooth transition that shows fast moving waves for intermediate values of the Larmor radius and had not been previously studied. The character of these fast waves is studied by decreasing the shock strength so nonlinear effects become small and linear wave analysis can be applied. The simulation results are Fourier analyzed to form a dispersion plot which is compared to the analytic dispersion relations from plasma wave theory. For the electromagnetic plasma shock problem the wave vector is perpendicular to the discontinuity and parallel to the longitudinal magnetic field. The plasma dispersion relation for this case yields the left and right circularly polarized waves (L mode and R mode), in addition to the slower Alfvén waves.

$$\frac{c^2k^2}{\omega^2} = 1 - \frac{\omega_{pe}^2}{\omega\left(\omega \pm \omega_{ce}\right)} \tag{21}$$

where $\omega_{pe} = \sqrt{n_e e^2/m_e\epsilon_o}$ is the electron plasma frequency and $\omega_{ce} = eB/m_e$ is the electron cyclotron frequency. The simulation and analytical results are shown in Fig. 3. The low frequency portion of the lower branch of the R mode is the whistler wave. The agreement of the numerical and analytical results supports the physical basis for the fast waves in the two-fluid simulations.

2.2.2 Multi-Dimensional Algorithm

The formulation of the approximate Riemann solver for the fluid equations allows for a straight forward extension to multiple dimensions. The extension from one to two dimensions introduces the complexity of extending the algorithm to multiple dimensions. The extension from two to three dimensions only requires additional compute resources but does not add additional complexity. Therefore, a large effort is concentrated on the two dimensional algorithm.

The divergence constraints on the magnetic and electric fields are satisfied automatically in one dimension and the electromagnetic fields are solved using an upwind characteristic-based method. However, in multiple dimensions the divergence constraints can be difficult to satisfy with the presence of current and charge sources on an arbitrary computational grid. The divergence constraints are satisfied by reformulating Maxwell's equations to include correction potentials.

The approach involves coupling the divergence constraint equations with the time-dependent field equations to form a perfectly hyperbolic equation set. [3] The field equations are expressed as

$$\frac{\partial \mathbf{B}}{\partial t} + \nabla \times \mathbf{E} + \gamma \nabla \psi = 0, \tag{22}$$

$$\frac{\partial \mathbf{E}}{\partial t} - c^2 \nabla \times \mathbf{B} + \chi c^2 \nabla \phi = -\frac{\mathbf{j}}{\epsilon_0}, \tag{23}$$

$$\frac{1}{\chi}\frac{\partial \phi}{\partial t} + \nabla \cdot \mathbf{E} = \frac{\rho_c}{\epsilon_0}, \tag{24}$$

$$\frac{1}{\gamma c^2}\frac{\partial \psi}{\partial t} + \nabla \cdot \mathbf{B} = 0, \tag{25}$$

where ϕ and ψ are the electric and magnetic correction potentials or, more formally, Lagrange multipliers which vanish at the domain boundaries. The method more accurately predicts the propagation speed of the waves; however, the method can overestimate the Lorentz force caused by charge separation. The implementation illustrates the importance of tightly coupling the field solver to the fluid solver.

Open or absorbing boundaries can be troublesome for finite volume methods applied to electromagnetic fields because the impedance mismatch causes spurious reflections and oscillations. The problem has been solved by implementation a PML (perfectly matched layer) boundary condition [21,22] which is common in PIC codes.

The two dimensional algorithm has been applied to the cylindrical electromagnetic plasma shock problem and the collisionless magnetic reconnection problem. The simulation results for the two-dimensional electromagnetic plasma shock are shown in Fig. 4. The fast waves have already left the domain by this time. The discontinuous jump in the out-of-plane magnetic field is supported by an azimuthal current carried primarily by the electron fluid. The electron fluid undergoes a Kelvin-Helmholtz instability which broadens the current layer. (This behavior may be important for shock degradation in hypersonic vehicles.) The simulation results from the collisionless magnetic reconnection problem are shown in Fig. 5. The simulation demonstrates an important numerical effect.

As described, the source terms make the equations stiff and must be treated implicitly to relax the stiffness. The relaxation works well for transient problems. However, for problems involving equilibrium conditions, the equilibrium force balance artificially diffuses resulting in a loss of the original equilibrium. The simulation ultimately reduces to a trivial equilibrium.

Magnetic reconnection is the process where plasma currents coalesce and magnetic fields reconnect. The process is demonstrated by a plasma sheet carrying an initially uniform current. The current produces oppositely directed magnetic fields above and below the plasma sheet. The plasma current supports the jump in the magnetic field, and the configuration is in force balance (equilibrium) though large forces are present. If the plasma has collisions (finite resistivity), the current sheet breaks into small filaments through a magnetic tearing instability. [23] However, even perfectly conducting plasmas undergo a similar instability that is due to two-fluid effects instead of resistivity. The current sheet again breaks into current filaments. The magnetic field reconnects "through" the remaining plasma sheet. The process is important in many applications including space physics. [24] However, it is a difficult problem to

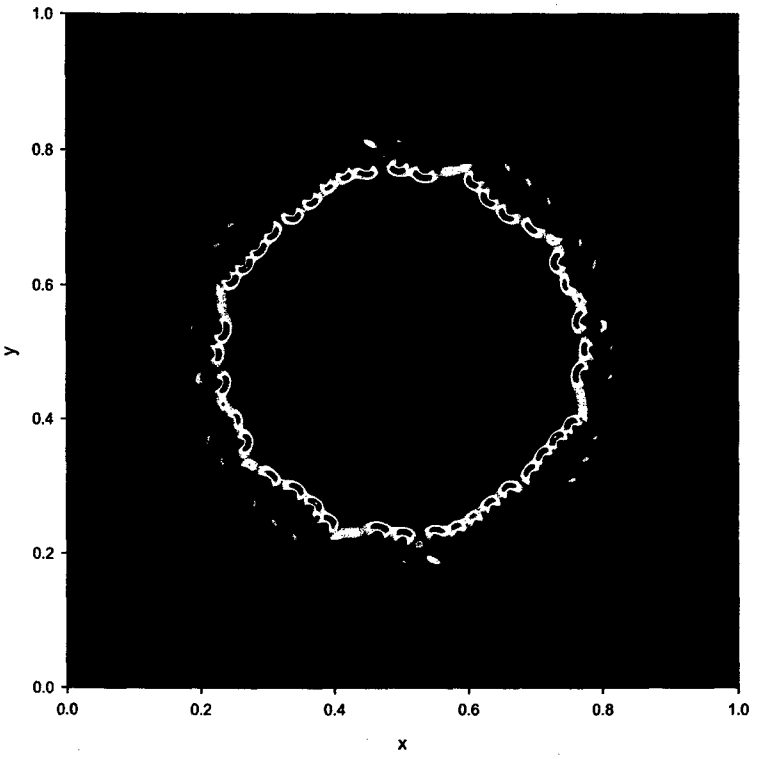

Figure 4: Two-dimensional electromagnetic plasma shock simulation showing the magnitude of in-plane electron current density. The azimuthal current supports the discontinuous jump in the out-of-plane magnetic field. The current layer is seen to broaden due into a turbulent layer due to a Kelvin-Helmholtz instability.

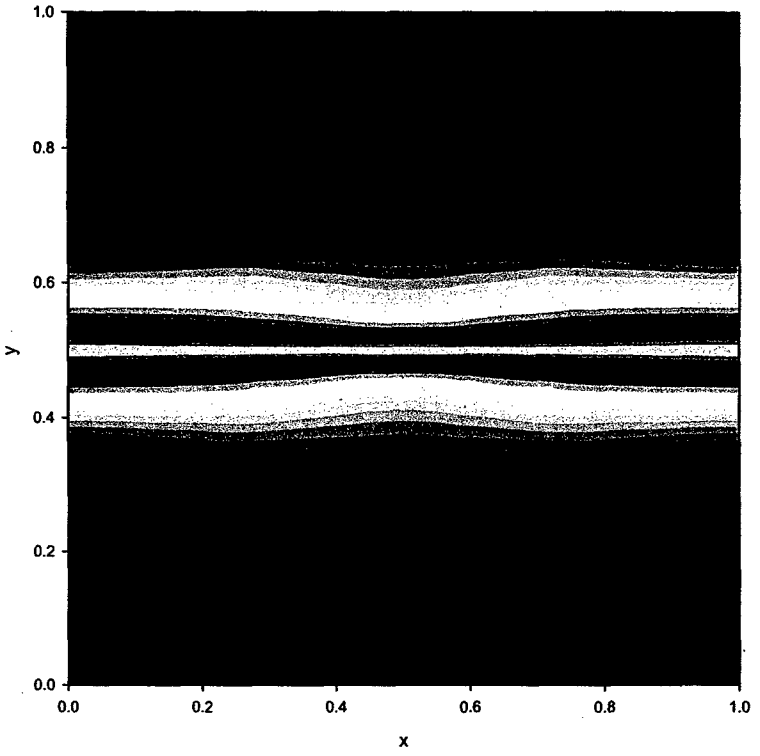

Figure 5: Magnetic field contours for the collisionless magnetic reconnection problem solved with the finite volume method. Shown is the magnitude of the transverse magnetic field B_x (parallel to the current sheet). The equilibrium jump in the magnetic field has diffused significantly.

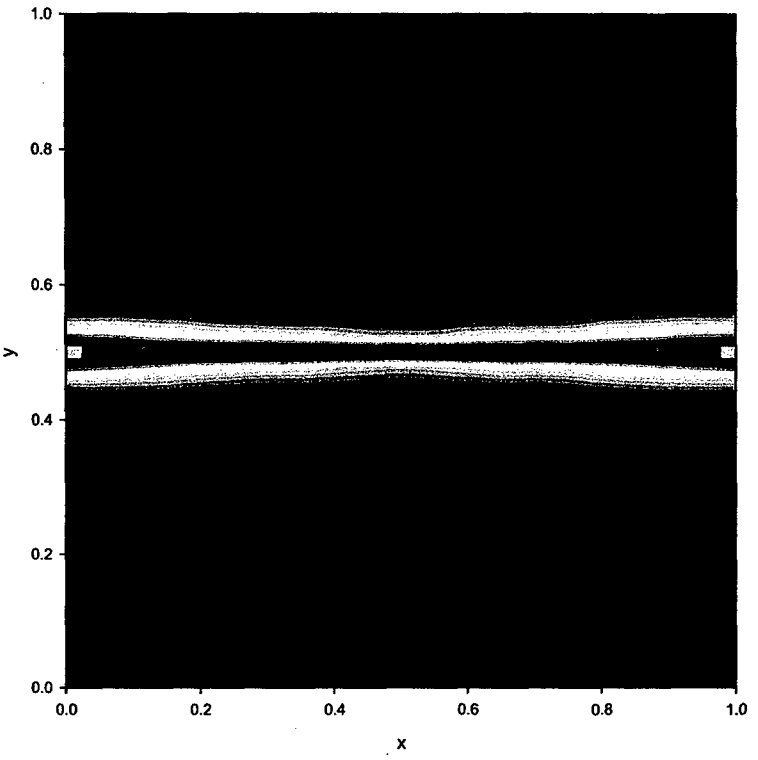

Figure 6: Magnetic field contours for the collisionless magnetic reconnection problem solved with a higher-order method. Shown is the magnitude of the transverse magnetic field B_x (parallel to the current sheet). The equilibrium jump in the magnetic field is maintained.

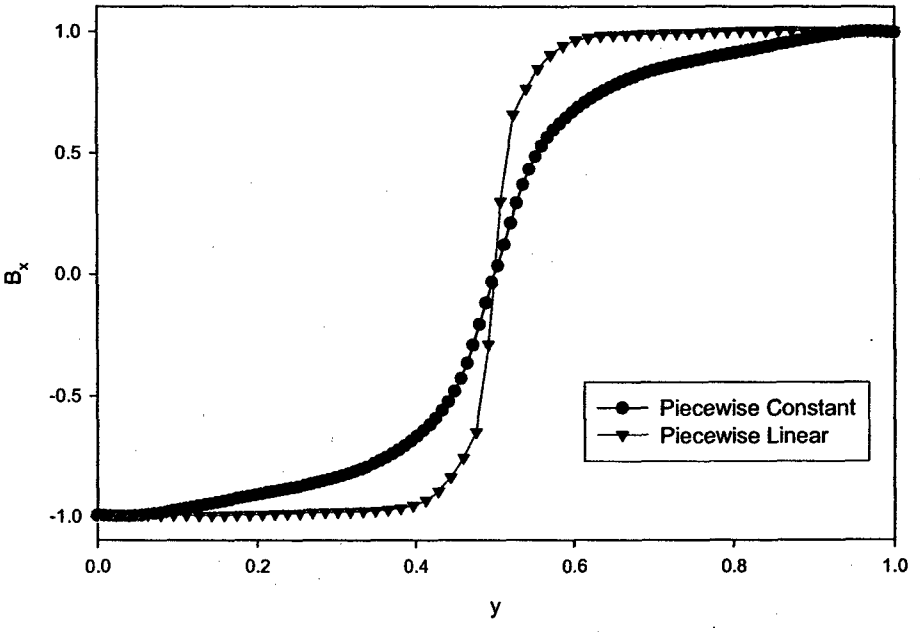

Figure 7: Comparison of the transverse magnetic field at $x = 0.5$ computed using the finite volume method and the higher order method. The higher order method better preserves the equilibrium jump in the magnetic field.

model and provides a rigorous test for the algorithm. Simulations of the two-dimensional collisionless reconnection problem are performed using the algorithm described previously with the implicit source treatment. Figure 5 shows the simulation results. Shown are contours of the magnitude of the transverse magnetic field B_x (parallel to the current sheet). The equilibrium jump in the magnetic field has diffused significantly.

Preliminary results using higher-order methods have solved the problem. [4] Figure 6 shows the same simulation of the two-dimensional collisionless reconnection problem using an algorithm that is second-order in space and third-order in time implemented for a uniform computational mesh. Figure 7 compares B_x through the domain midplane as computed by the previous method and the higher-order method. The higher-order method preserves the equilibrium jump in the magnetic field. The higher-order algorithm uses a discontinuous Galerkin method with a TVD Runge-Kutta time advance. [25–27]

The conserved variables of the two-fluid plasma model are modeled with a set of basis functions, $\{v_h\}$. The governing equations, expressed as eqn (17), are multiplied by each basis function and integrated over the mesh cell volume Ω. An integral equation is generated for each basis function.

$$\int_\Omega v_h \frac{\partial Q}{\partial t} dV + \oint_{\partial\Omega} v_h \mathbf{F} \cdot d\mathbf{S} - \int_\Omega \mathbf{F} \cdot \nabla v_h dV = \int_\Omega v_h S dV \tag{26}$$

where the divergence theorem has been applied to the second term. The volume and surface integrals are replaced with Gaussian quadrature. The flux $\mathbf{F}$ is computed with the approximate Riemann solver with a limiter applied directly to the conserved variables to get high resolution. The source terms are described by the basis functions and are, therefore, the same order accurate as the solution variables. This satisfies the higher order accuracy requirement to preserve the equilibrium balance between the divergence of the flux and the source.

For the preliminary, two-dimensional, second-order accurate algorithm, a linear set of basis functions are used.

$$\{v_h\} = \{v_0, v_x, v_y\} = \left\{1, \frac{x - x_{ij}}{\Delta x/2}, \frac{y - y_{ij}}{\Delta y/2}\right\} \tag{27}$$

where the center of the mesh cell is located at (x_{ij}, y_{ij}) and extends Δx by Δy. The conserved variables Q are defined as

$$Q = Q_0 + Q_x v_x + Q_y v_y \tag{28}$$

within each mesh cell. Update equations for the coefficients for each conserved variable are found directly from eqn (26) applied to each mesh cell.

The temporal evolution is determined with a Runge-Kutta method.

The preliminary discontinuous Galerkin method has greatly reduced the diffusion of the equilibrium forces. Figure 6 shows the same simulation of the two-dimensional collisionless reconnection problem using an algorithm that is second-order in space and third-order in time. Figure 7 compares B_x through

the domain midplane as computed by the previous method and the higher order method. The higher order method preserves the equilibrium jump in the magnetic field.

References

[1] P. L. Roe. *Journal of Computational Physics*, 43:357, 1981.

[2] U. Shumlak and J. Loverich. Approximate Riemann solver for the two-fluid plasma model. *Journal of Computational Physics*, 187:620–638, 2003.

[3] C. D. Munz, P. Ommes, and R. Schneider. A three-dimensional finite volume solver for the Maxwell equations with divergence cleaning on unstructured meshes. *Computer Physics Communications*, 130:83–117, 2000.

[4] J. Loverich and U. Shumlak. A discontinuous Galerkin method for the full two-fluid plasma model. *Computer Physics Communications*, 169:251–255, 2005.

[5] G. H. McCall, J. A. Corder, and the USAF Scientific Advisory Board. *New World Vistas, Air and Space Power for the 21st Century.* United States Air Force Document, 1995.

[6] A. R. Bell. Computational Simulation of Plasmas. *Astrophysics and Space Science*, 256:13–35, 1998.

[7] C. Z. Cheng and G. Knorr. *Journal of Computational Physics*, 22:330, 1976.

[8] H. Ruhl and P. Mulser. *Physics Letters A*, 205:388, 1995.

[9] L. Chacón, D. C. Barnes, D. A. Knoll, and G. H. Miley. *Journal of Computational Physics*, 157:618, 2000.

[10] L. Chacón, D. C. Barnes, D. A. Knoll, and G. H. Miley. *Journal of Computational Physics*, 157:654, 2000.

[11] C. K. Birdsall and A. B. Langdon. *Plasma Physics via Computer Simulation.* McGraw-Hill, New York, 1985.

[12] J. P. Freidberg. Ideal magnetohydrodynamic theory of magnetic fusion systems. *Reviews of Modern Physics*, 54(3):801–902, July 1982.

[13] R. E. Peterkin Jr., M. H. Frese, and C. R. Sovinec. Transport of Magnetic Flux in an Arbitrary Coordinate ALE Code. *Journal of Computational Physics*, 140(1):148–171, February 1998.

[14] U. Shumlak, T. W. Hussey, and R. E. Peterkin Jr. Three-Dimensional Magnetic Field Enhancement in a Liner Implosion System. *IEEE Transactions on Plasma Science*, 23(1):83–88, February 1995.

[15] O. S. Jones, U. Shumlak, and D. S. Eberhardt. *Journal of Computational Physics*, 130:231, 1997.

[16] B. Udrea and U. Shumlak. Nonlinear study of spheromak tilt instability. In *AIAA 36th Aerospace Sciences Meeting & Exhibit*, Reno, Nevada, January 1998. AIAA Paper No. 98-0995.

[17] R. E. Peterkin and P. J. Turchi. Magnetohydrodynamic theory for hypersonic plasma flow - what's important and what's not. In *AIAA 31st Plasmadynamics and Lasers Conference*, Denver, Colorado, June 2000. AIAA Paper No. 2000-2257.

[18] D. Harned and Z. Mikic. *Journal of Computational Physics*, 83:1, 1989.

[19] J. T. Becerra Sagredo. Semi-implicit treatment of the hall term in finite volume, mhd computations. Master's thesis, University of Washington, Seattle, WA 98195, June 1998.

[20] M. Brio and C. C. Wu. *Journal of Computational Physics*, 75:400, 1988.

[21] E. Turkel and A. Yefet. Absorbing pml boundary layers for wave-like equations. *Applied Numerical Mathematics*, 27:533–557, 1998.

[22] F. Bonnet and F. Poupaud. Berenger absorbing boundary condition with time finite-volume scheme for triangular meshes. *Applied Numerical Mathematics*, 25:333–354, 1997.

[23] H. P. Furth, J. Killen, and M. N. Rosenbluth. Finite-resistivity instabilities of a sheet pinch. *Physics of Fluids*, 6(4):459–484, April 1963.

[24] J. Birn, J. F. Drake, M. A. Shay, B. N. Rogers, R. E. Denton, M. Hesse, M. Kuznetsova, Z. W. Ma, A. Bhattacharjee, A. Otto, and P. L. Pritchett. Geospace Environmental Modeling (GEM) Magnetic Reconnection Challenge. *Journal of Geophysical Research*, 106(2):3715, 2001.

[25] B. Cockburn and C.-W. Shu. *Mathematics of Computation*, 52:411, 1989.

[26] B. Cockburn, S. Hou, and C.-W. Shu. *Mathematics of Computation*, 54:545, 1990.

[27] B. Cockburn and C.-W. Shu. *Journal of Computational Physics*, 141:199, 1998.